Anti-Cancer Drugs 1994, **5**, pp. 539–547

Pharmacokinetic studies on Elobromol in children with brain tumors

Christine Paál,[1] Valéria Erdélyi-Tóth,[2] Éva Pap,[2] Csilla Csáki,[1] Thomas Ferencz,[1] Dezső Schuler[1] and Joseph D Borsi[1]

[1]Second Department of Pediatrics, Semmelweis Medical School, Budapest, Tuzolto u. 7–9, 1094, Hungary. Tel: (+36) 1 215 1985; Fax: (+36) 1 215 9969. [2]National Institute of Oncology, Budapest, Rath Gyorgy u. 7–9, 1122, Hungary.

Systemic pharmacokinetics of high dose (500 mg/m^2), orally administered Elobromol (dibromodulcitol, DBD) were studied in 16 chemotherapeutic courses administered to five patients. Cerebrospinal fluid (CSF) DBD levels were also analyzed in two patients. Bromoepoxydulcitol (BED), dianhydrodulcitol (DAD) are cytotoxic, whereas bromoanhydrodulcitol (BAD) and anhydroepoxydulcitol (AED) are inactive metabolites detectable during the biotransformation of DBD. The HPLC method, developed by our team, is suitable for the determination of both DBD and its main metabolites (DAD and BAD). Our publication is the first in the literature to describe the pharmacokinetic properties of these three hexitol derivatives in pediatric patients. With the exception of one patient, concentration time curves were analyzed by the one-compartment model. From 30 min following administration, DBD was detectable in all plasma samples for at least 12 h; its concentration, however, was usually undetectable by 24 h. Though highly variable in value, DAD concentrations were detectable during all but one of the therapeutic courses. The following peak concentrations were observed: DBD = 3.46–30.63 μM, DAD = 1.70–6.17 μM and BAD = 0–5.63 μM. The correlation of AUC_{BAD} and AUC_{DBD} values were exponential up to 200 μM h with no additional increase detectable above this limit: the distribution of AUC_{BAD} and AUC_{DBD} was described by a maximum curve. The possibility of enterohepatic recirculation could not be excluded for any of the compounds studied. Each of the three hexitol derivatives was detectable in CSF even if the concentration of the individual metabolite remained undetectable in plasma. DBD CSF concentrations were almost constant in the period from 2.5 to 8 h following administration. Due to rising DAD concentrations, however, the value of the CSF/plasma concentration ratio was >1. The cumulation of the inactive BAD metabolite in CSF was also significant.

Key words: Brain tumor, children, dibromodulcitol, pharmacokinetics.

Introduction

During the last four decades, research on antineoplastic preparations in Hungary has yielded a number of alkylating sugar-alcohol derivatives. Chemical and pharmacological properties, mode of action and clinical application of dibromodulcitol (1, 6-dibromo-dulcitol (DBD), Elobromol, Mitolactol)—the most prominent member of this series—have been discussed in more than 250 publications.[1] Though numerous trials were conducted to determine the therapeutic value of DBD in various neoplastic conditions developing in adults, pediatric application of the preparation was evaluated by Sitarz[2,3] and Schuler[4–6] only. As the penetration of DBD through the blood–brain barrier is highly significant,[7–10] it has been incorporated into therapeutic protocols for patients with brain tumors.[5,6,11–13]

Due to its poor water solubility, DBD can be administered by the oral route only. The metabolites produced during its biotransformation[10,14] have been identified by previous *in vitro* solvolytic studies.[15] Its bifunctional epoxyde-derivative metabolites—bromoepoxydulcitol (BED) and dianhydrodulcitol (1,2-5,6-dianhydrodulcitol, DAD)—possess antineoplastic activity;[16,17] however, its monofunctional derivatives—bromoanhydrodulcitol (1-bromo-3,6-anhydrodulcitol, BAD) and anhydroepoxydulcitol (AED)—lack biological activity.[18]

DBD is a weak alkylating agent with a phase-specific effect on malignant cells. Its effect is maximal on tumor cells in the G_1 phase of the cell cycle;[19] whereas the antineoplastic activity of DAD is the greatest on cells in the late S phase of the cycle.[20] DBD–DNA interaction studies were invaluable for interpreting the mode of action of this compound.[21] According to Jeney,[22] DBD binds first to chromosomal proteins, then to DNA.[23] The interaction of DBD with DNA results in the formation of mono- and diguanine alkyl-derivatives substituted at position 7.[24]

CC is a fellow of the Hungarian Academy of Sciences. TF is a fellow of the Agency of International Development of the USA. This work was supported by the Hungarian Scientific Research Foundation (OTKA), Foundation for the Hungarian Sciences and the USA AID POOH program.

Correspondence to JD Borsi

Pharmacokinetic data from animal experiments[8,25,26] as well as from studies conducted in adults[10–14,27–29] are abundant. Initial results in the pediatric age group have been reported from our laboratory.[5]

The present study has been conducted to define the pharmacokinetic properties of DBD, a component of the medulloblastoma protocol developed at our department (Table 1) with the purpose of obtaining reliable data for adjustments of dose and frequency of administration if it is necessary.

Materials and methods

As neither the concentration of DBD nor that of its derivatives can be determined by direct techniques, several indirect methods have been developed.[9,10,30] Modifying the method of Henner *et al.*[30] we have developed a method for the simultaneous determination of DBD and its metabolites (DAD and BAD) in plasma and cerebrospinal fluid (CSF).

The original method of Henner *et al.*[30] used 500 µl of plasma which was mixed with 2 volumes of ice-cold methanol and incubated at −20°C for 20 min. After centrifugation (1500 *g* for 5 min), 1 ml of supernatant was mixed with 1 ml of 5% diethyldithiocarbamate and 2 ml of 50 mM potassium phosphate (pH 7.4). Following incubation at 50°C for 1 h, the derivative was extracted into 5 ml chloroform. Then, a 4 ml portion of the chloroform extract was dried under nitrogen at 40°C. Chromatography was performed on an Altech CN column (5 µm particles, 25 × 0.46 cm), the mobile phase consisted of a mixture of 74.4% heptane, 21.6% isopropyl-alcohol and 4% glacial acetic acid. The flow rate was 1.3 ml/min, the detection wavelength was 254 nm and the retention time was 9.9 min. This method made it possible to determine only the sum of the DBD, bromoepoxydulcitol and DAD, and was unable to measure the BAD concentrations. Our method needs double the amount of plasma but is able to determine the exact concentrations of the biotransformational products as well after a shorter reaction time.

Materials

Elobromol as well as the standard preparations used for the validation of pharmacokinetic studies (DBD, BAD and DAD) were supplied by Chinoin Pharmaceuticals. With the exception of *n*-heptane (supplied by the Carlo Erba Co., Milan, Italy), reagents and chemicals were Reanal (Budapest, Hungary) products of HPLC grade.

Chromatography system

HPLC was performed using a Beckman System Gold HPLC instrument (equipped with a Beckman System Gold 116 pump and a 166 detector), a 5 µm 250 × 4 mm Spherisorb CN column connected with a 20 × 4 mm guard column. The composition of the eluent was 750 ml *n*-heptane, 174.5 ml isopropyl-alcohol, 74.5 ml glacial acetic acid and 50 µl triethyl-amine; at a flow rate of 0.9 ml/min. The injected volume was 20 µl. Quantitative DBD, DAD and BAD analysis was performed with an adjustable wavelength UV detector at 254 nm by measuring the area under the peak of the chromatography curve. Data were processed automatically by a computer connected to the HPLC system. Plasma and CSF samples were analyzed after plasma and phosphate buffered calibration, respectively.

Preparation of samples

Either 2000 or 1500 µl ice-cold methanol was added to 1000 µl plasma or to 500 µl liquor, respectively. Plasma proteins were removed by centrifuging the mixture at 2000 *g* for 10 min in a cooled centrifuge. Then, 800 µl aliquots of the supernatant were separated for the determination of DBD + DAD − BAD and DAD concentrations (see below).

***A**: DBD + DAD–BAD determination.* Supernatant (800 µl) was mixed with 1000 µl 5% sodium diethyldithiocarbamate (DDTC) dissolved in water. Following incubation at 55°C for 25 min the derivative was extracted into 4 ml chloroform. A 3 ml portion from the organic phase was dried under nitrogen at 40°C.

***B**: DAD determination.* Supernatant (800 µl) was mixed with 750 µl 0.05 N potassium dihydrogen phosphate (pH 7.4) and 250 µl 5% DDTC solution. Following incubation at 18°C for 40 min the derivative was extracted into 4 ml chloroform. A 3 ml portion from the organic phase was dried under nitrogen at 40°C.

The rest of the mixtures were refrigerated at −20°C for further measurements scheduled for the next day. Samples were dissolved in 150 µl eluent before HPLC determination.

Quantitative analysis

The retention time (t_R) of the BAD derivative (1-diethyldithiocarbamoil-3,6-anhydrodulcitol) in our chromatography system was 7.9 min in reaction **A**. The derivatives of DBD and DAD were identical (1,6-bis[diethyldithiocarbamoil]-dulcitol) and were represented by a common peak (t_R = 9.6 min). The exact amount of DAD was performed in reaction **B**, as—due to its lower reactivity under such conditions—DBD did not react with DDTC. The concentration of unchanged DBD was therefore calculated by subtracting the results of reaction **B** from **A**.

The detection limit was 0.5 μM for each of the monitored compounds.

Human plasma from healthy volunteers was spiked with known amounts of the three hexitol derivatives to determine the recoveries. These at the concentration range of 2–50 μM were: DBD, 94–105%; DAD, 70–98%; BAD, 83–110%.

Pharmacokinetic calculations

The results of the measurements were processed by MedUSA software (version 1.5/1.587; CheMicro Ltd, Budapest). Concentration–time paired data were analyzed by fitting one- and two-compartment models with first-order absorption for the distribution of orally administered drugs.

The equation of the one-compartment model is

$$c(t) = D/Vk_a[\exp(-k_e(t - t_{lag}))] - [\exp(-k_a(t - t_{lag}))]/(k_a - k_e) \quad (1)$$

The equation of the two-compartment model is

$$c(t) = A\exp[-\alpha(t - t_{lag})[-B\exp[-\beta(t - t_{lag})] + K\exp[-k_a(t - t_{lag}) \quad (2)$$

where $K = -(A + B)$

The software calculated the following pharmacokinetic parameters: area under the concentration–time curve by the trapezoidal rules method with the extrapolation from the final data point to infinity (AUC); the lagtime (t_{lag}); biological half-life ($t_{1/2ka}$, $t_{1/2ke}$); calculated peak plasma concentration (c_{max}) and the time needed for its development (t_{max}); systemic clearance (Cl); mean residence time (MRT) and the steady state volume of distribution (V_{ss}). As the low water solubility of the active substance excluded its parenteral administration, clearance values were calculated assuming a bioavailability of 1 ($F = 1$) and are therefore estimates only.

AUC was calculated up to the last data point by the trapezoidal method using the Pharmacological Calculations software (Version 4.0).

Treatment protocol

Patients received a combination of chemotherapy, irradiation and surgery according to the medulloblastoma therapy protocol developed at our department. Therapy and the collection of samples were undertaken in compliance with the Geneva nomenclature and with the written consent of parents/relatives. Cytotoxic drugs prescribed in the protocol for the postoperative period are listed in Table 1.

Patients

In the period from 1 December 1992 to 1 June 1993, the pharmacokinetic properties of high-dose (500 mg/m^2) oral Elobromol were investigated in five patients (during 16 therapeutic courses) at the Second Department of Pediatrics, Semmelweis Medical School. In two patients, diagnostic spinal taps created the opportunity to determine drug concentrations in the CSF on four occasions. All patients were female, with a mean age of 7.4 ± 4.3 years. The data of the patients are detailed in Table 2.

Collection of samples

The drug was taken after a light breakfast. Due to the condition of the fourth patient, Elobromol was administered in suspension (mixed with feeding formula) through a nasogastric tube.

Blood samples were drawn through an indwelling cannule, before as well as 0.5, 1, 1.5, 2, 2.5, 3, 3.5, 4, 5, 6, 7, 8, 12 and 24 h after the oral administration of high-dose Elobromol. Blood was drawn into heparinized tubes and was separated immediately. CSF specimens were collected by lumbar puncture. Unprocessed plasma and CSF samples were refrigerated at −20°C.

Results

Pharmacokinetic studies of DBD administered according to the therapeutic protocol (Table 1) were performed on weeks 1, 2 and 3 in three patients (patients 1–3), and weeks 1 and 2 in patient 4. In the case of the fifth patient, DBD pharmacokinetics

Table 1. Medulloblastoma protocol

Drug	Dose	Route of administration	Time of treatment(week)
Vincristin	1.5 mg/m^2, maximum 2 mg	i.v.	weeks 1–2, 19–20, 29–30, 38–39 (on the first day of the week)
Elobromol (dibromodulcitol)	500 mg/m^2	orally	weeks 1–3, 19–21, 29–31, 38–40 (on the first day of the week)
Natulan (procarbazine)	100 mg/m^2/day	orally	weeks 1–3, 19–21, 29–31, 38–40
Methotrexate with leucovorin rescue	5 g/m^2/24 h according to the serum MTX levels	24 h infusion i.v. or orally	week 4
Methotrexate	according to the age	i.th.	at the end of the 24 h infusion
Vepesid (etoposide)	100 mg/m^2	i.v. 1 h infusion	week 4 on the day of methotrexate administration and the day after
Radiotherapy	tumor dose 55 Gy craniospinal dose 30 Gy		from week 7 to 13
Elobromol (dibromodulcitol)	50 mg/m^2/day	orally	from week 7 to 13 during the radiotherapy
Vepesid (etoposide)	50 mg/m^2	i.v. bolus	weeks 15, 24, 34
Platidiam (cisplatin)	90 mg/m^2/5 h	5 h infusion	weeks 15, 24, 34

Table 2

Patient	Diagnosis	Age (years)	Time of the pharmacokinetic examination (week of the treatment)	Time of drawing CSF samples
1	medulloblastoma	11	1, 2, 3	weeks 1 and 3 (at 2.5 h) week 2 (at 3 h)
2	ependymoma	4	1, 2, 3	
3	primitive neuroectodermal tumor (PNET)	2	1, 2, 3	week 1 (at 8 h)
4[a]	medulloblastoma	8	1, 2	
5[b]	medulloblastoma	12	19, 30, 31, 39, 40	

[a] Due to the condition of the patient, crushed tablets were administered suspended in feeding formula in both instances.
[b] The therapy scheduled for week 3 was cancelled due to the condition of the patient. The number of the high dose Elobromol treatments was thus reduced from 12 to 11 by the end of the protocol. However, as the patient was released from the hospital in good general condition, on weeks 39 and 40 samples were collected for 6 h after drug administration only.

were studied at weeks 19, 30, 31, 39 and 40 of therapy.

In patients 1 and 3, diagnostic spinal taps provided the opportunity for determining drug concentrations in the CSF. Pharmacokinetic properties of both DBD and its metabolites (DAD and BAD) were studied.

DBD in plasma

The most important pharmacokinetic parameters determined by calculation are listed in Tables 3–6. AUC values shown were generated by infinite extrapolation by the trapezoidal rules method.

In the majority of the pharmacokinetic studies performed, concentration–time curves for DBD were calculated by the one-compartment model.

DBD was present in measurable concentrations in the plasma in all patients from 30 min after administration and during the next 12 h. DBD levels were already undetectable by 24 h in most cases.

Analysis of the majority of the curves raised the possibility of enterohepatic recirculation. As can be seen in Figures 1 and 2, there was a further concentration elevation after the first peak concentration.

Table 3. Pharmacokinetic parameters of DBD during the first week of therapy (the parameters of patient 1 were calculated by the two-compartment model)

Pharmacokinetic parameter	Patient 1	Patient 2	Patient 3	Patient 4	Mean ± SD
$t_{1/2(ka)}$ (h)	1.17	1.67	1.19	1.53	1.39 ± 0.25
$t_{1/2(\alpha)\ (ke)}$ (h)	1.37	1.89	1.23	1.53	1.51 ± 0.28
$t_{1/2(\beta)}$ (h)	32.91				
t_{lag} (h)	1.56	0.03	0.76	0.34	0.67 ± 0.66
c_{max} calculated (μM)	28.17	3.60	15.40	7.97	13.79 ± 10.76
t_{max} calculated (h)	3.54	2.59	2.51	2.55	2.80 ± 0.50
AUC (trap.) (μM h)	437.68	32.09	73.54	55.06	149.59 ± 192.81
AUC_{BAD}/AUC_{DBD}	0.17	0.08	0.56	0.25	0.26 ± 0.21
AUC_{DAD}/AUC_{DBD}	0.03	0.65	0.48	0.74	0.48 ± 0.31

Table 4. Pharmacokinetic parameters of DBD during the second week of therapy (the parameters of patient 4 were calculated without fitting a curve, directly from the measured values using the trapezoidal rules method)

Pharmacokinetic parameter	Patient 1	Patient 2	Patient 3	Patient 4	Mean ± SD
$t_{1/2(ka)}$ (h)	1.89	1.01	1.99		1.63 ± 0.54
$t_{1/2(ke)}$ (h)	9.16	1.76	2.00		4.31 ± 4.20
t_{lag} (h)	0.49	0.38	0.91		0.59 ± 0.28
c_{max} calculated (μM)	19.61	10.45	10.10		13.39 ± 5.39
t_{max} calculated (h)	3.38	2.28	3.78		3.15 ± 0.78
AUC (trap.) (μM h)	285.65	74.74	86.49	58.54	126.36 ± 106.81
AUC_{BAD}/AUC_{DBD}	0.30	0.00	0.14	0.12	0.14 ± 0.12
AUC_{DAD}/AUC_{DBD}	0.00	0.42	0.38	0.83	0.41 ± 0.34

Table 5. Pharmacokinetic parameters of DBD during the third week of therapy

Pharmacokinetic parameter	Patient 1	Patient 2	Patient 3	Mean ± SD
$t_{1/2(ka)}$ (h)	1.56	4.33	0.48	2.12 ± 1.99
$t_{1/2(ke)}$ (h)	4.21	4.00	1.99	3.40 ± 1.23
t_{lag} (h)	0.48	0.38	0.18	0.35 ± 0.15
c_{max} calculated (μM)	14.35	6.68	11.14	10.72 ± 3.85
t_{max} calculated (h)	4.02	5.74	1.47	3.74 ± 2.15
AUC (trap.) (μM h)	152.00	102.45	54.35	102.93 ± 48.83
AUC_{BAD}/AUC_{DBD}	0.54	0.00	0.00	0.18 ± 0.31
AUC_{DAD}/AUC_{DBD}	0.52	0.50	0.52	0.51 ± 0.01

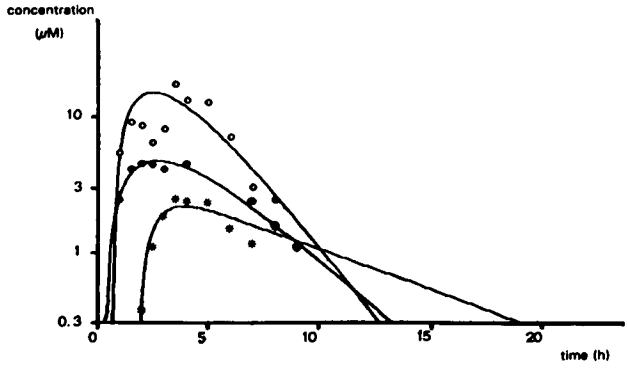

Figure 1. DBD (○), DAD (●) and BAD (*) concentrations determined during the first treatment of patient 3.

Special comments on individual patients

Patient 1. DBD plasma concentration–time data obtained during the first treatment of patient 1 was best described by the two-compartment model. Accuracy of the analysis of the data obtained during the second treatment was identical irrespective of applying either the one- or the two-compartment model (perfection of interpolation $r^2 = 0.924$ for both models). The characteristics of data from the third treatment justified the application of the one-compartment model. AUC_{DBD} values were greater during all 3 weeks of therapy than the correspond-

Table 6. Pharmacokinetic parameters of DBD in the case of patient 5 during weeks 19–40

Pharmacokinetic parameter	Week 19	Week 30	Week 31	Week 39	Week 40
$t_{1/2(ka)}$ (h)	2.84	1.87	4.20	0.98	1.54
$t_{1/2(ke)}$ (h)	2.83	1.87	4.27	1.59	2.19
t_{lag} (h)	1.18	0.77	1.33	1.13	0.36
c_{max} calculated (μM)	12.65	5.27	7.44	6.41	9.65
t_{max} calculated (h)	5.26	3.47	7.43	2.91	2.99
AUC (trap.) (μM h)	173.23	35.89	132.74	30.51	64.54
AUC_{0-6} (trap.) (μM h)	61.14[a]	22.07	22.69	24.97	42.58
AUC_{BAD}/AUC_{DBD}	0	0	0.135	0	0.059
AUC_{DAD}/AUC_{DBD}	0.08	0.70	0.19	1.03	1.50
AUC_{BAD}/AUC_{DBD} (0–6 h)	0	0	0.23	0	0.10
AUC_{DAD}/AUC_{DBD} (0–6 h)	0.02[a]	0.47	0.34	0.98	0.44

As on weeks 39 and 40 samples were collected for 6 h after drug administration only, AUC values calculated for the period 0–6 h are given for comparison as well.
[a] On week 19 the drawing of the 6 h specimen was thwarted by technical reasons. Thus AUC values are given for the period 0–7 h instead of 0–6 h.

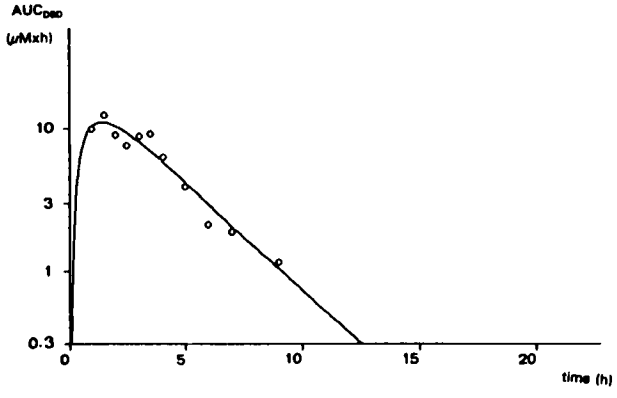

Figure 2. Possibility of enterohepatic recirculation at 3–5 h in DBD plasma samples of patient 3.

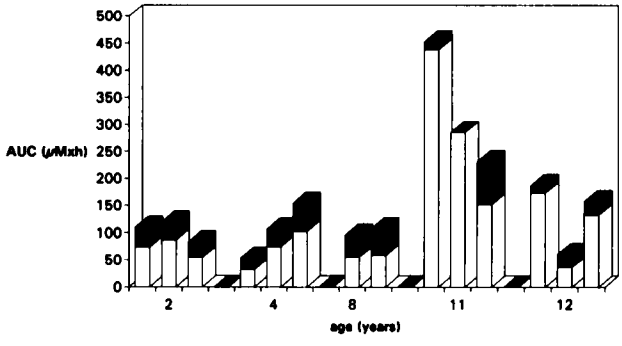

Figure 3. Age-dependent changes of AUC values of the total cytostatically active agents (DBD and DAD) during the consecutive treatments. ■, AUC (DAD); □, AUC (DBD).

ing values of other patients for the same treatment period.

Patient 3. Figure 1 shows the fitted curves generated by applying the one-compartment model to the plasma concentration-time series of patient 3 on the first week of therapy.

Patient 4. In the case of this patient, DBD was administered through a nasogastric tube. After the first week of therapy, the pharmacokinetic curve of this patient was identical to those of the others. On the second week of treatment, however, plasma levels were almost constant throughout the period from 30 min after administration to 24 h without discernible absorption or elimination phases. Therefore fitting of the appropriate curves was not possible.

Patient 5. The AUC of the 0–6 h section of the concentration–time curve of patient 5 is given for comparison in Table 6. The AUC_{DBD} values of this patient were also greater in later weeks of treatment. As patients 1 and 5 were comparable in age and the oldest in this patient group, the correlation of AUC_{DBD} and AUC_{DAD} values with age was also analyzed (Figure 3).

BAD in plasma

BAD was present in detectable concentrations in the plasma of all patients during the first week of treatment; these data were analyzed by the one-compartment model, but was undetectable in the plasma of patient 2 after the second treatment; in the plasma of patients 2 and 3 during the third week; and of patient 5 during weeks 19, 30 and 39. When insuf-

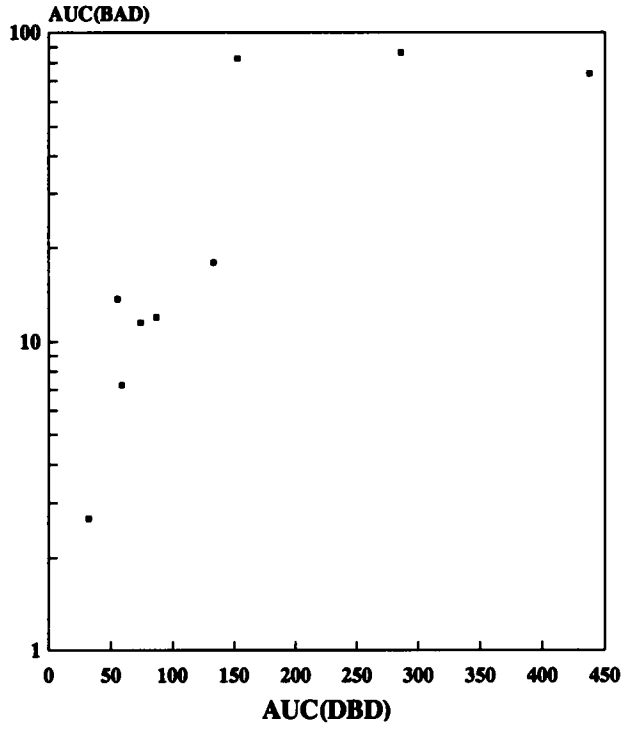

Figure 4. The relation of BAD and DBD AUC values.

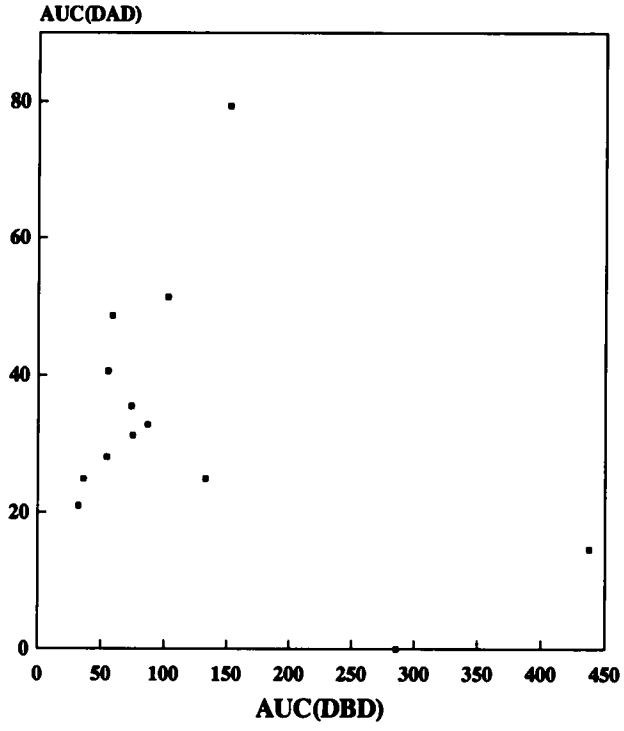

Figure 5. The relation of DAD and DBD AUC values.

ficient number of the measurable concentration data points did not allow us to fit a curve, AUC_{BAD} could be calculated using the trapezoidal rules method. The calculated AUC value ratios refering to DBD are collected in Tables 3–6.

The value of AUC_{BAD} was increasing exponentially with that of AUC_{DBD} up to a limit of 200 μM h. Further elevation of AUC_{DBD} values was not followed by any increase in AUC_{BAD} (Figure 4). In six cases, where BAD was undetectable in serum, AUC_{DBD} was in the range of 0–200 μM h.

DAD in plasma

DAD was not found in detectable quantities only in the plasma of patient 1 during the second week of treatment. Despite this, however, DAD was present in the CSF of the patient.

When the insufficient number of the measurable concentration data points did not allow us to fit a curve, AUC_{DAD} could be calculated using the trapezoidal rules method. The calculated AUC value ratios referring to DBD are collected in Tables 3–6.

Plotting AUC_{DBD} against AUC_{DAD} revealed a maximum curve distribution (Figure 5).

Concentrations in the CSF

Table 7 depicts the CSF and corresponding plasma concentrations and their ratios.

Discussion

Although several authors[8,10,14,27,29] have already published their results on the pharmacokinetics of DBD–DAD, methods of determination and the doses applied are different.

The modified HPLC method made the simultaneous determination of DBD and its metabolites (DAD and BAD) possible in plasma and CSF.

Plasma concentration–time data pairs were predominantly interpolated by applying the one-compartment model. The substances studied appeared in the plasma after the elapse of a lag-period: 0.03–1.56 h for DBD; BAD appeared usually later than DAD, in five from the nine cases when there was detectable amounts of both BAD and DAD. Peak plasma concentrations were as follows: DBD = 3.46–30.63 μM; DAD = 1.70–6.17 μM; BAD = 1.39–5.63 μM. The time necessary for the development of the peak DBD concentration was in the range from 1.5 to 5 h.

Table 7. DBD, DAD and BAD concentrations in the CSF, corresponding plasma concentrations and calculated CSF/plasma ratio

	Time (h)	CSF levels (μM)			Plasma levels (μM)			Liquor plasma concentration ratio		
		DBD	BAD	DAD	DBD	BAD	DAD	DBD	BAD	DAD
Patient 1 on week 1	2.5	1.01	0.37	0.92	20.13	3.54	0.48	0.05	0.11	1.92
Patient 1 on week 2	3	0.89	0.49	1.54	19.94	3.53	0	0.04	0.14	
Patient 1 on week 3	2.5	0.76	0	0.41	13.05	2.59	0	0.06		
Patient 3 on week 1	8	1.62	3.30	3.45	2.48	1.58	1.61	0.65	2.09	2.14

DAD concentrations of patient 1 on the third week was 0.41 μM; in the plasma, however, DAD became detectable from 5 h only.

The presumed time of enterohepatic recirculation is reflected by the section between 5 and 7 h for DBD curves, 6 and 7 h for DAD curves, and 5 and 9 h for BAD curves.

The evaluation of t_{lag} values suggests that absorption of the drug begins in the stomach. The extremely high inter- and intra-individual variability of numeric data reflects differences in absorption, due to varying contents of the stomach, to the status of intestinal mucosa and to several other factors not yet elucidated.

With the exception of samples taken during the second treatment of patient 1, both DBD and DAD were detectable in the plasma of all patients. The quantity of BAD, however, showed great variability with the progression of therapy. AUC_{BAD} values decreased in patients 2–4, but increased in patient 5 as a possible consequence of AUC_{DBD} elevation.

The AUC_{DBD} related changes of DAD and BAD as well as their alterations with repeated treatments may indicate that these compounds are produced by enzymatic processes and not by solvolysis.

Though neither the possibility of age-related decreases in AUC_{DBD} nor the role of decreasing metabolism can be ruled out, these presumptions can be proven by further investigations only. The failure to detect DAD in the serum of adult patients,[28,29] however, seems to be in favor of the above hypotheses.

The analysis of CSF samples has demonstrated that all three dulcitol derivatives enter this compartment even if their corresponding plasma concentration remains below the detectable limit at the same time. Being cytotoxic components, the presence of DBD and DAD in the CSF is an essential component of therapeutic efficacy. The increase in their relative CSF/plasma ratio during the period from 2.5 to 8 h after administration (Table 7) is a highly remarkable observation. DBD concentrations in CSF were low during the period from 2.5 to 3 h (0.76–1.01 μM). However, despite the exponential reduction of plasma levels, its value remained at least relatively stable until 8 h. The DAD concentration was between 0.41 and 1.54 μM in 2.5–3 h CSF samples and increased to 3.45 μM by 8 h (Table 7). The value of the CSF/plasma ratio was already greater than 1 in the 2.5 h samples. This reflects the significant accumulation of the drug in CSF—an extraordinary feature among the cytotoxic drugs known so far. Our study provided preliminary information on the pharmacokinetics of a drug that may have an important role in the treatment of childhood brain tumors. Further studies are planned in our institution to evaluate the relationship between the pharmacokinetics and pharmacodynamics of DBD and its metabolites.

References

1. Eckhardt S, ed. *Dibromodulcitol.* Budapest: Medicina Konyvkiado 1982.
2. Sitarz AL, Albo V, Movassagi N, *et al.* Incidence of CNS leukemia in children with ALL or AML receiving cytoxan or didromobulcitol for remission maintenance. *Proc Am Ass Cancer Res* 1974; **15**: 48.
3. Sitarz AL, Albo V, Movassagi N, *et al.* Dibromodulcitol (NSC-104800) compared with cyclophosphamide (NSC-26271) as remission maintenance therapy in previously treated children with acute lymphoblastic leukemia or undifferentiated leukemia: possible effectiveness in reducing the incidence of central nervous system leukaemia. *Cancer Chemother Rep* 1975; **59**: 989–94.
4. Schuler D, Kardos G, Révész T. Dibromodulcitol containing chemotherapeutic regimen in the treatment of childhood Hodgkin's disease. *Neoplasma* 1988; **35**: 599–603.
5. Schuler D, Smoló P, Koós R, *et al.* Treatment of malignant scala posterior brain tumors in children: The chemotherapy of relapsed medulloblastoma with a dibromodulcitol containing drug regimen and pharmacokinetic studies of dibromodulcitol in children. *Med Ped Oncol* 1992; **20**: 312–4.
6. Schuler D, Somló P, Koós R, *et al.* The treatment of malignant scala posterior tumors in children. II: preliminary results of the pre- and postoperative adjuvant chemotherapy of scala posterior tumors. *Med Ped Oncol* 1993; **21**: 274–9.

7. Belej MA, Troetel WM, Weiss AJ, *et al.* The absorption and metabolism of Dibromodulcitol in patients with advanced cancer. *Clin Pharmacol Ther* 1972; **13**: 563–72.
8. Institóris L, Dzurillay E, Pethes G. Comparative studies on the *in vivo* distribution pattern of dibromodulcitol and diepoxydulcitol. *Z Krebsforsch* 1973; **79**: 49–57.
9. Eckhardt S, Csetényi J, Horváth IP, *et al.* Uptake of labelled dianhydrogalactitol into human gliomas and nervous tissue. *Cancer Treat Rep* 1977; **61**: 841–7.
10. Horváth IP, Csetényi J, Hindy I, *et al.* Metabolism and Pharmacokinetics of Dibromodulcitol (DBD, NSC-104800) in man II. Pharmacokinetics of DBD. *Eur J Clin Cancer Clin Oncol* 1982; **18**: 1211–9.
11. Retsas S, Gershuny AR. Central nervous system involvement in malignant melanoma. *Cancer* 1988; **61**: 1926–34.
12. Levin VA, Wheeler KT. Chemotherapeutic approaches to brain tumors. Experimental observations with dianhydrogalactitol and dibromodulcitol. *Cancer Chemother Pharmacol* 1982; **8**: 125–31.
13. Levin VA, Edwards MSB, Gutin PH, *et al.* Phase II evaluation of dibromodulcitol in the treatment of recurrent medulloblastoma, ependymoma, and malignant astrocytoma. *J Neurosurg* 1984; **61**: 1063–8.
14. Horváth IP, Csetényi S, Kerpel-Fronius S, *et al.* Metabolism and pharmacokinetics of Dibromodulcitol (DBD, NSC-104800) in man. I. Metabolites of DBD. *Eur J Cancer* 1979; **15**: 337–44.
15. Vidra I, Simon K, Institóris I, *et al.* The chemical transformation products of 1,6-dibromo-1,6-dideoxygalactitol and 1,2-5,6-dianhydrogalactitol in aqueous solution. *Carbohydr Res* 1982; **111**: 41–57.
16. Horváth IP, Somfai-Relle S, Hegedûs L, *et al.* Toxicity, antitumour and haematological effects of 1,-anhydro-6-bromogalactitol and D-mannitol: a comparison with the related dibromo- and dianhydro-derivatives. *Eur J Cancer Clin Oncol* 1982; **18**: 573–7.
17. Elson LA, Jarman M, Ross WCJ. Toxicity, haematological effects and anti-tumour activity of epoxides derived from disubstituted hexitols. Mode of action of mannitol myleran and dibromomannitol. *Eur J Cancer* 1968; **4**: 617–25.
18. Somfai-Relle S, Németh L. Antitumour effect of DBD *in vivo*. In Eckhardt S, ed. *Dibromodulcitol.* Budapest: Medicina Konyvkiado 1982.
19. Oláh E, Pályi I, Sugár J. Effects of cytostatics on proliferating and stacionary cultures of mammalian cells. *Eur J Cancer* 1978; **14**: 895–900.
20. Pályi I. Survival and phase sensitivity of HeLa cells treated with dianhydrogalactitol (NSC-132313). *Cancer Chemother Rep* 1975; **59**: 493–9.
21. Institóris E, Somfai Zs, Vargai Z, *et al.* Interaction of dibromo- and dianhydrodulcitol with chromatin constituents of tumor cells. In Siegenthaler W, Lüthy R, eds. *Current chemotherapy.* Washington: American Society for Microbiology 1978: **II**; 1305–8.
22. Jeney A, Dzurillay É, Lapis K, *et al.* Chromatin proteins as a possible target for antitumour agents: alterations of chromatin proteins in dibromodulcitol treated Yoshida tumours. *Chem-Biol Interact* 1979; **26**: 349–61.
23. Jeney A, Szabó I, Vályi-Nagy T, *et al.* Pharmacobiochemical studies on cytotoxic polyol derivatives. II. The effect of biological alkylating agents on the thermaldenaturation properties of DNA. *Eur J Cancer* 1970; **6**: 297–302.
24. Institóris E, Tamás J. The formation of alkylated bases in DNA by a bifunctional alkylating agent, dianhydrogalactitol. *Proc 5th Meeting of European Association for Cancer Res*, Vienna 1979.
25. Intsitóris L, Horváth IP, Pethes G. Some characteristic features of the biotransport of the cytostatic agent 1,6-dibromo-1,6-dideoxydulcitol. *Int J Cancer* 1967; **2**: 21–6.
26. Gáti É, Horváth IP, Kralovánszky J, *et al.* Studies on the metabolism of dibromodulcitol in rats bearing Yoshida ascites tumours. In: *Proc 7th Int Congr of Chemotherapy*, Prague, 1971.
27. Horváth IP, Csetényi S, Kerpel-Fronius S, *et al.* Pharmacokinetics and metabolism of dianhydrogalactitol DAG in patients: a comparison of dibromodulcitol DBD. *Eur J Cancer Oncol* 1986; **22**: 163-71.
28. Gyergyay F, Kerpel-Fronius S, Erdélyi-Tóth V, *et al.* Dibromodulcitol (DBD) and 5-Fluorouracil (5-FU) combination chemotherapy of cervical cancer. Phase I study. In *Proc 16th Int Congr of Chemotherapy*, Israel, 1989.
29. Kelley S, Peters PW, Andersen J, *et al.* Pharmacokinetics of dibromodulcitol in humans: A Phase II. Study. *J Clin Oncol* 1986; **4**: 753–61.
30. Henner WD, Furlong EA, Kelley SL, *et al.* Assay for Mitolactol and its bifunctional alkylating metabolites in plasma. *J Pharm Sci* 1985; **74**: 983–6.

(Received 14 April 1994; received in revised form 5 July 1994; accepted 21 July 1994)